

The charge ordered state in half-doped Bi-based manganites studied by ^{17}O and ^{209}Bi NMR

A.Trokiner,¹ S.Verkhovskii,^{1,2} A.Yakubovskii,^{1,3,4} K.Kumagai,⁴ S-W.Cheong,⁵ D.Khomskii,⁶ Y.Furukawa,⁴ J.S.Ahn,⁵ A.Pogudin,² V.Ogloblichev,² A.Gerashenko,² K.Mikhalev,² and Yu.Piskunov²

¹ *Laboratoire de Physique du Solide, E.S.P.C.I., Paris, France*

² *Institute of Metal Physics, Ural Branch of Russian Academy of Sciences, Ekaterinburg GSP-170, Russia*

³ *Russian Research Centre "Kurchatov Institute", Moscow, Russia*

⁴ *Division of Physics, Graduate School of Sciences, Hokkaido University, Sapporo, Japan*

⁵ *Department of Physics and Astronomy, State University of New Jersey, Rutgers, USA*

⁶ *II Physikalisches Institut, Universitaet zu Koln, Germany*

(Dated: August 30, 2018)

We present a ^{209}Bi and ^{17}O NMR study of the Mn electron spin correlations developed in the charge ordered state of $\text{Bi}_{0.5}\text{Sr}_{0.5}\text{MnO}_3$ and $\text{Bi}_{0.5}\text{Ca}_{0.5}\text{MnO}_3$. The unusually large local magnetic field $^{209}H_{loc}$ indicates the dominant $6s^2$ character of the lone electron pair of Bi^{3+} -ions in both compounds, probably, responsible for the high temperature of charge ordering T_{CO} . The observed difference in $^{209}H_{loc}$ for $\text{Bi}_{0.5}\text{Sr}_{0.5}\text{MnO}_3$ to $\text{Bi}_{0.5}\text{Ca}_{0.5}\text{MnO}_3$ is suggested to be due to a decrease in the canting of the staggered magnetic moments of Mn^{3+} -ions from adjacent ab layers. The modification of the ^{17}O spectra below T_{CO} demonstrates that the NMR line due to the apical oxygens is a unique local tool to study the development of the Mn spin correlations. In the AF state the analysis of the ^{17}O spectrum of $\text{Pr}_{0.5}\text{Ca}_{0.5}\text{MnO}_3$ and $\text{Bi}_{0.5}\text{Sr}_{0.5}\text{MnO}_3$ points towards two different types of charge ordering in these systems: a site-centered for the first manganite and a bond-centered one for the second material.

PACS numbers: 75.30.Et, 76.60.Cq

I. INTRODUCTION

Among doped transition metal oxides, one of the most interesting systems to study charge ordering (CO), orbital ordering (OO), and spin ordering phenomena is the half-doped manganites $\text{R}_{0.5}\text{A}_{0.5}\text{MnO}_3$ (R - rare-earth ion or Bi; A - Ca, Sr). Furthermore, manganites show the colossal magnetoresistance effect which results from the competition between the insulating charge-ordered state and metallic ferromagnetic state. Nevertheless, the role of charge ordering and/or orbital ordering in the magnetotransport properties of manganites remains unclear.

At high temperature $\text{R}_{0.5}\text{A}_{0.5}\text{MnO}_3$ is in the charge-disordered (CD) paramagnetic (PM) state. The disorder is related to the thermally activated hopping of e_g -holes. This hopping causes ferromagnetic (FM) correlations between the electron spins of the neighboring Mn-ions,^{1,2,3} the spin-fluctuation parameters being controlled by the double-exchange mechanism proposed by Zener.⁴ Below T_{CO} the localization of the mobile holes induces transition to the CO phase. The spatial ordering of electrons over given Mn-orbitals leads to an excess in the kinetic energy that is compensated by the elastic energy due to the cooperative Jahn-Teller distortions in the MnO_6 -octahedra sublattice. The orbital ordering is related to the Jahn-Teller distortions.

In the present work, OO and CO have been studied in Bi-based manganites. The critical temperature of charge ordering is $T_{CO} = 325$ K for $\text{Bi}_{0.5}\text{Ca}_{0.5}\text{MnO}_3$ ⁵ and 475 K for $\text{Bi}_{0.5}\text{Sr}_{0.5}\text{MnO}_3$.⁶ One open problem is why the critical temperature of charge ordering T_{CO} in Bi-based manganites is so much higher than in their

rare-earth counterparts. It was established for the rare-earth manganites $\text{RE}_{0.5}(\text{Ca},\text{Sr})_{0.5}\text{MnO}_3$ that the e_g -band width is controlled by the (Mn-O-Mn)-bond bending which in turn depends on $\langle r_A \rangle$ - the average radius of (RE,A)-cations. A smaller $\langle r_A \rangle$ narrows e_g -band and favors the hole localization thus increasing T_{CO} . Recently it was shown,⁶ that such correlation between T_{CO} and $\langle r_A \rangle$ is not observed in Bi-based manganites $\text{Bi}_{0.5}(\text{Ca}_{1-x},\text{Sr}_x)_{0.5}\text{MnO}_3$. While T_{CO} increases smoothly with $\langle r_A \rangle$ for $x \leq 0.4$ these manganites belong to one of the $Pbnm$ space subgroups in the CO-phase. The Sr-rich manganites ($x \geq 0.6$) belong to $Ibmm$ space subgroup and show the opposite tendency, i.e. T_{CO} decreases with $\langle r_A \rangle$.^{7,8,9} Thus, the high values of T_{CO} for $\text{Bi}_{0.5}\text{Ca}_{0.5}\text{MnO}_3$ and $\text{Bi}_{0.5}\text{Sr}_{0.5}\text{MnO}_3$ cannot be properly explained considering only the average buckling of the (Mn-O-Mn)-bonds. It was suggested⁶ that an increase of $6s^2$ character in the stereoactivity of the Bi^{3+} lone electron pair could favor the growth of T_{CO} for $x > 0.5$ but the mechanism of the influence of lone pairs, as well as the detailed orbital structure of these pairs in different Bi manganites, have not been clarified.

We have performed ^{209}Bi zero-field NMR measurements on $\text{Bi}_{0.5}\text{Ca}_{0.5}\text{MnO}_3$ and $\text{Bi}_{0.5}\text{Sr}_{0.5}\text{MnO}_3$ in the AFM-ordered state. According to Ref. 10, below the Neel temperature ($T_N \approx 155$ K) $\text{Bi}_{0.5}\text{Sr}_{0.5}\text{MnO}_3$ exhibits a static spin order of the CE' -type (see Fig. 1). For $\text{Bi}_{0.5}\text{Ca}_{0.5}\text{MnO}_3$ in the AFM state the magnetic structure ($T_N \approx 140$ K) has not been reported yet. For both compounds, we have observed a very large value of $^{209}H_{loc}$, the local field at Bi. It depends on the short-range spin order of the nearest Mn. For both samples

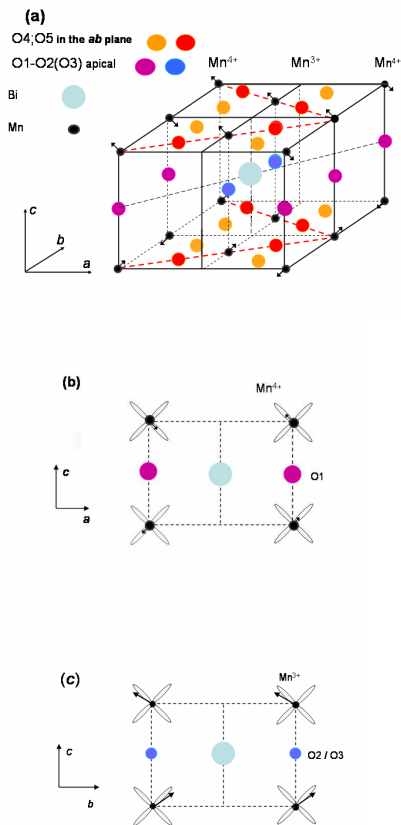


FIG. 1: CE'-type magnetic structure of $\text{Bi}_{0.5}\text{Sr}_{0.5}\text{MnO}_3$ ¹⁰ represented in the frame of a pure ionic model (site-centered order). The 3D structure is represented in (a). The red dotted lines show the ferromagnetically correlated zig-zag of Mn^{3+} and Mn^{4+} ions in the ab planes. The environment of Bi cation in the ac plane (b) and in the bc plane (c) is represented with the $\text{Mn}-t_g$ orbital orientation and the spin direction of the four nearest Mn ions, Mn^{4+} and Mn^{3+} , respectively. The (O1 - O5) sites of oxygen are specified similar to the notation suggested in Ref. 11.

the analysis of $^{209}\text{H}_{loc}$ has been performed in the frame of the CE'-type magnetic order, although it is not known for $\text{Bi}_{0.5}\text{Ca}_{0.5}\text{MnO}_3$. Our results favors the $6s$ dominant character of the lone pair of Bi rather than the $6p$ one. To ascertain magnetic structure of $\text{Bi}_{0.5}\text{Ca}_{0.5}\text{MnO}_3$ the ^{17}O NMR spectra were measured in zero external magnetic field at low temperature.

The purpose of the ^{17}O NMR study reported in this paper is to trace the Mn-Mn electron spin correlations which develop when cooling $\text{Bi}_{0.5}\text{Ca}_{0.5}\text{MnO}_3$ and $\text{Bi}_{0.5}\text{Sr}_{0.5}\text{MnO}_3$ in the CD/CO PM phase. In the first NMR investigation of the CO state of a half-doped manganite,³ it was shown that the ^{17}O NMR probe is a powerful tool to study the orbital ordering and the spin ordering. Compared to other techniques, NMR is a local probe, which enables us to obtain valuable information on the spin correlation of Mn-ions through the orbital

hybridization of Mn with the probed oxygen nucleus. Indeed it was shown by ^{17}O NMR³ that in $\text{Pr}_{0.5}\text{Ca}_{0.5}\text{MnO}_3$ the CE-type magnetic correlations develop gradually below T_{CO} . The AF correlations between the ab -layers appear first, and only at a lower temperature the CE-correlations in the ab -planes are formed. In this work we compare the formation of the Mn-Mn spin correlations in Bi-based manganites to that in $\text{Pr}_{0.5}\text{Ca}_{0.5}\text{MnO}_3$.

For half-doped manganites two possible scenario of CO/OO-transition are considered. The first relates to the localization of holes at e_g -orbital of the transition metal cation. It results in the conventional CE-order of the ions of different valence ($\text{Mn}^{3.5+\delta}/\text{Mn}^{3.5-\delta}$) in the ab -plane.^{12,13} This scenario is based on an ionic description of the charge ordering, it is also named site-centered.¹⁴

The second scenario suggests the formation of the Zener-polaron state, which consists of FM-correlated dimers of $\text{Mn}^{3.5+}$ -ions.¹⁵

This option is also named bond centered.¹⁴ The relation between the kinetic energy of the electrons in the e_g -band and the ab -plane superexchange coupling of t_g -electrons defines, in many respects, which type of CO is formed in a crystal.^{14,16} The details of CO in manganites are still an open question. Nevertheless, it was suggested in the x -ray diffraction study⁹ performed on a single crystal of $\text{Bi}_{0.5}\text{Sr}_{0.5}\text{MnO}_3$ that the CO-state in this system is formed by Zener pairs. We address the questions concerning the detailed form of the CO phase by studying the relative intensity of the lines in the ^{17}O spectra measured for the completely formed AF-CO state of manganites.

II. EXPERIMENT

We used powder samples of $\text{Bi}_{0.5}\text{Ca}_{0.5}\text{MnO}_3$ ($T_{CO} = 330$ K)⁶ and $\text{Bi}_{0.5}\text{Sr}_{0.5}\text{MnO}_3$ ($T_{CO} = 475$ K),⁶ which were prepared by the standard solid state reaction technique. The powders were enriched in ^{17}O isotope up to $\approx 20\%$. The single-phase nature of the enriched samples was confirmed by x -ray diffraction at room temperature.

The NMR measurements were performed with several commercial and home-built pulse phase-coherent NMR spectrometers operated in the frequency range 20 - 500 MHz using a spin-echo technique. The ^{209}Bi and ^{17}O NMR spectra were obtained by measuring at each frequency (ν) the intensity, $^{209}\text{Int}(\nu)$, of the spin-echo signal formed with the radio-frequency (rf) pulse sequence $(\pi/2) - t - (\pi)$. The width of a $(\pi/2)$ rf -pulse did not exceed $(1.5 - 2) \mu\text{s}$. The ^{17}O NMR signal in H_2O was used as the frequency reference (ν_0) to determine the shift of NMR line $K = (\nu - \nu_0)/\nu_0$.

The measurements of the broad ^{17}O NMR spectra in the antiferromagnetic state (see Section D) were performed with a special care. We used a single NMR coil for the whole frequency range. Its quality factor Q was chosen smoothly dependent on the frequency ν . At each frequency the impedance of the resonance circuit was

matched to the 50 Ohm input impedance of the receiver, and the gain of the rf power amplifier was adjusted to the maximum of the echo intensity, ^{17}Int , keeping the width of the $(\pi/2)$ rf -pulse constant. Such a care had to be paid in order to provide at every point of the broad spectrum the echo-signal voltage, $V(t=0)$, which is proportional to spectral intensity the ^{17}O NMR spectrum multiplied by ν^2 . The spectral intensity normalized in such a manner yields the fraction of oxygen contributing to the echo at the given frequency point.

III. RESULTS AND DISCUSSION

A. ^{209}Bi zero-field NMR spectra

Figure 2 shows the ^{209}Bi NMR spectra measured in the AFM-ordered state of $\text{Bi}_{0.5}\text{Ca}_{0.5}\text{MnO}_3$ ($T_N = 140$ K)⁵ and $\text{Bi}_{0.5}\text{Sr}_{0.5}\text{MnO}_3$ ($T_N = 155$ K)⁹ in zero external magnetic field (ZFNMR) at $T = 4.2$ K. The spectral intensity of the very broad line of ^{209}Bi (nuclear spin $^{209}I = 9/2$, quadrupolar moment $^{209}Q = -0.35$ barns) is presented as the echo intensity, $^{209}\text{Int}(\nu)$, corrected by the factor ν^{-2} . The components of the local magnetic field ($^{209}H_{loc}$) as well as the parameters of electric field gradient (EFG, V_{ii}) - quadrupole frequency, $^{209}\nu_Q = e^2QV_{ZZ}/21$, and asymmetry parameter, $^{209}\eta = (V_{XX} - V_{YY})/V_{ZZ}$ with $|V_{ZZ}| \geq |V_{XX}| \geq |V_{YY}|$, - were determined from the exact diagonalization of the Hamiltonian, including both the magnetic and the electric quadrupole interactions of the ^{209}Bi nuclei with the corresponding local magnetic field and EFG. The calculation was performed for the matrix representation in the frame of reference, XYZ, where the corresponding term of electric quadrupole interaction is diagonal. The calculated transitions $\Delta m_I = 1; 2$ are indicated by narrow peaks in Fig. 2 and the corresponding results for $^{209}H_i$, $^{209}\nu_Q$ and $^{209}\eta$ are listed in Table I. We have taken into account distributions of both $^{209}H_{loc}$ and the EFG parameters, that can appear due to the Bi/Sr or Bi/Ca charge disorder. The distribution functions were taken in the Gaussian form with the corresponding width δH_{loc} and $\delta \nu_Q$. The calculated broadened spectrum representing the result of such a convolution is drawn by the grey curve in Fig. 2. With a single set of NMR parameters it reproduces the experimental data points rather well in a wide frequency range.

The line of central transition $m_I = -1/2 \longleftrightarrow +1/2$ peaks at $\nu_0 = 80$ MHz for $\text{Bi}_{0.5}\text{Sr}_{0.5}\text{MnO}_3$ and at $\nu_0 = 65$ MHz for $\text{Bi}_{0.5}\text{Ca}_{0.5}\text{MnO}_3$. It corresponds to a very large local magnetic field at the Bi-site in the AFM-state $^{209}H_{loc} = 101$ kOe and $^{209}H_{loc} = 85$ kOe in $\text{Bi}_{0.5}\text{Sr}_{0.5}\text{MnO}_3$ and $\text{Bi}_{0.5}\text{Ca}_{0.5}\text{MnO}_3$, respectively. For comparison, the local field at ^{139}La nuclei is $^{139}H_{loc} = 3.5$ kOe in the AFM ordered LaMnO_3 .¹⁷ Moreover, in the FM-ordered domains of the half-doped $\text{La}_{0.5}\text{Ca}_{0.5}\text{MnO}_3$ the fully polarized eight nearest Mn moments create at

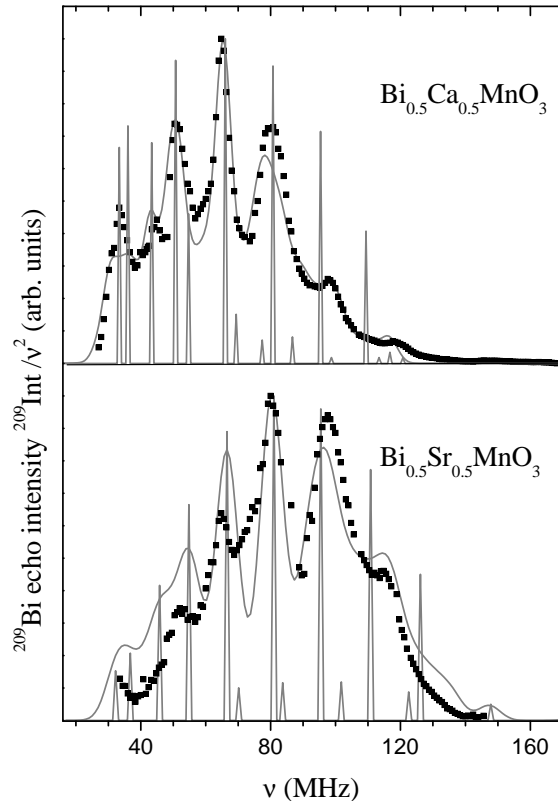


FIG. 2: Zero-field ^{209}Bi NMR spectra in $\text{Bi}_{0.5}\text{Ca}_{0.5}\text{MnO}_3$ and $\text{Bi}_{0.5}\text{Sr}_{0.5}\text{MnO}_3$ measured by spin-echo technique at 4.2 K. The echo intensity ^{209}Int (solid squares) is plotted versus the frequency ν . The set of narrow peaks shows the calculated transitions with the parameters given in Table I. The grey curve is the calculated broadened spectrum assuming a gaussian distribution for both the local field $^{209}H_{loc}$ and the quadrupole frequency ν_Q (see text for details).

TABLE I: Parameters of the calculated ^{209}Bi zero-field NMR spectra shown in Fig. 1. See text for the definition of the X, Y and Z components of $^{209}H_{loc}$. δH_{loc} and $\delta \nu_Q$ are the width of the gaussian distribution of the magnetic and quadrupolar interactions, respectively.

Sample	$\text{Bi}_{0.5}\text{Sr}_{0.5}\text{MnO}_3$	$\text{Bi}_{0.5}\text{Ca}_{0.5}\text{MnO}_3$
$^{209}H_{loc}$ (kOe)	101(5)	85(5)
H_X (kOe)	9	0
H_Y (kOe)	37	33
H_Z (kOe)	94	78
δH_{loc} (kOe)	10	6
ν_Q (MHz)	16(1)	14(1)
$\delta \nu_Q$ (MHz)	3	3
η	0.90(5)	0.75(5)

the ^{139}La the field $^{139}H_{loc} = 36.3$ kOe^{18,19}, which is much

less than those observed in this study.

Two types of magnetic order, namely A-type and CE'-type magnetic structures were revealed at $T = 1.5$ K in neutron diffraction studies of polycrystalline $\text{Bi}_{0.5}\text{Sr}_{0.5}\text{MnO}_3$.¹⁰ The A-type magnetic order should result in the complete cancellation of $^{209}\text{H}_{loc}$ at the Bi-site similar to the situation of La-site in LaMnO_3 .¹⁷ For CE'-type, the AFM-order leads to a net transfer of spin polarization from the four neighboring Mn^{3+} -ions to Bi (see Fig. 1 c).

The resulting local field is aligned along [001] direction and its magnitude is proportional to $|\mu_c(\text{Mn}^{3+})|$ - the c-projection of the staggered magnetic moment of Mn^{3+} . For further comparison of different hyperfine couplings it is more convenient to consider the local field $^{209}\text{h}_{loc}$ created at the Bi-nuclei by one electron spin. By specifying $|\mu_c(\text{Mn}^{3+})| = 1.4 \mu_B$ ¹⁰ we obtain

$$^{209}\text{h}_{loc} = ^{209}\text{H}_{loc}/[4|\mu_c(\text{Mn}^{3+})|] = 18.2\text{kOe}/\mu_B, \quad (1)$$

for $\text{Bi}_{0.5}\text{Sr}_{0.5}\text{MnO}_3$ with the CE'-type AFM-order. This value exceeds more than four times the corresponding value of $^{139}\text{h}_{loc} = 4.5 \text{ kOe}/\mu_B$ found in $\text{La}_{0.5}\text{Sr}_{0.5}\text{MnO}_3$ at the FM state.¹⁸

It is worth noting that in the insulating state of manganites the $6sp$ -orbital of La^{3+} -ion is nearly empty, while the Bi^{+3} -ion holds two electrons at the $6sp$ valence shell. As it was suggested in Ref. 18, the $6s$ -orbital of the La^{3+} cation can hybridize with one of the three $t_{2g}(\text{Mn})$ atomic orbitals with a single unpaired spin. In the Bi-based manganites the similar $t_{2g}(\text{Mn})$ - $6s(\text{Bi})$ overlap is one of the possible ways to transfer $3d$ -electron spin polarization of Mn-ions to the central Bi-cation. Another possibility is the Mn spin polarization transfer via $e_g(\text{Mn})$ - $2p(\text{O})$ - $6p(\text{Bi})$ orbitals but it seems less effective in providing a local field comparable in magnitude with the observed one. Indeed, the corresponding hyperfine field due to the core polarization $H_{cp}(6p) \sim 300 \text{ kOe}$ per electron is approximately two orders of magnitude less than the Fermi contact hyperfine field $H_{FC}(6s) \sim 10^4 \text{ kOe}$ per electron.²⁰ The former case would lead to an unrealistic high value of the p -wave spin polarization f_{6p} , which is transferred from Mn to the $6p$ -orbital of Bi - $f_{6p} = ^{209}\text{h}_{loc}/H_{cp}(6p) \approx 0.15$. In the case of $t_{2g}(\text{Mn})$ - $6s(\text{Bi})$ overlap, the large Fermi-contact field $H_{FC}(6s)$ yields a much more reasonable estimate of the corresponding transferred $6s$ -wave spin polarization $f_{6s} = ^{209}\text{h}_{loc}/H_{FC}(6s) \approx 0.004$.

Thus, taking into account the large Fermi-contact hyperfine field created at the nuclei by a single unpaired electron located at the $6s$ -orbital, $H_{FC}(6s)$, one can suggest that the observed very large $^{209}\text{H}_{loc}$ strongly favors the dominant $6s$ character rather than the p character of the lone electron pair of Bi in both $\text{Bi}_{0.5}\text{Sr}_{0.5}\text{MnO}_3$ and $\text{Bi}_{0.5}\text{Ca}_{0.5}\text{MnO}_3$.

We do not think that the reduced value of $^{209}\text{H}_{loc}$ in $\text{Bi}_{0.5}\text{Ca}_{0.5}\text{MnO}_3$ compared to $\text{Bi}_{0.5}\text{Sr}_{0.5}\text{MnO}_3$ is due to a change in $s^2 \rightarrow sp/p^2$ character of the Bi lone electron pair as suggested in Ref. 6, since the decrease is not as

large as expected for such change when considering the values of $H_{FC}(6s)$ and $H_{cp}(6p)$.

The difference in the observed $^{209}\text{H}_{loc}$ is more probably due to variation of the canting of the staggered magnetic moments of Mn^{3+} ions in $\text{Bi}_{0.5}\text{Ca}_{0.5}\text{MnO}_3$ compared with $\text{Bi}_{0.5}\text{Sr}_{0.5}\text{MnO}_3$ as shown below. As the magnetic structure of the AFM state in $\text{Bi}_{0.5}\text{Ca}_{0.5}\text{MnO}_3$ at low temperature has not been reported yet we make an attempt to clarify this point by measuring ^{17}O ZFNMR in the same samples at 4.2K.

B. ^{17}O Zero Field NMR spectra

Figure 3 shows the zero field ^{17}O NMR (ZFNMR) spectra in the AFM ordered state of $\text{Pr}_{0.5}\text{Ca}_{0.5}\text{MnO}_3$ (a), $\text{Bi}_{0.5}\text{Ca}_{0.5}\text{MnO}_3$ (b), and $\text{Bi}_{0.5}\text{Sr}_{0.5}\text{MnO}_3$ (c) oxides at 4.2 K.²⁵

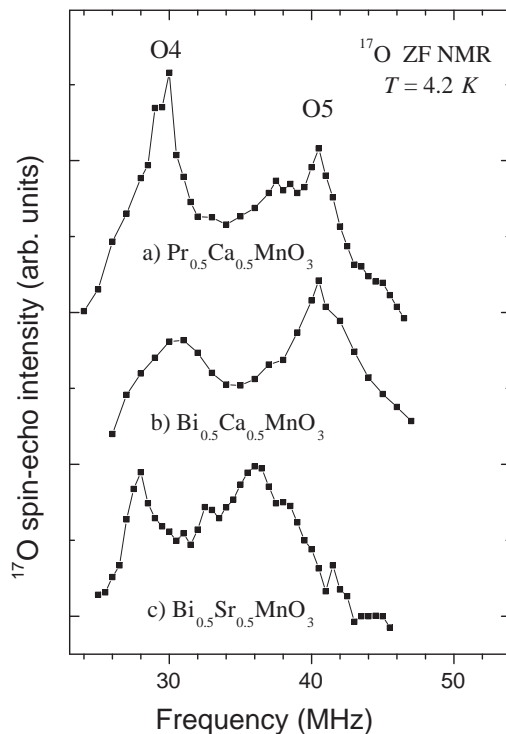


FIG. 3: Zero-field ^{17}O NMR spectra measured at 4.2 K in the antiferromagnetic charge ordered state of $\text{Pr}_{0.5}\text{Ca}_{0.5}\text{MnO}_3$ (a) $\text{Bi}_{0.5}\text{Ca}_{0.5}\text{MnO}_3$ (b) and $\text{Bi}_{0.5}\text{Sr}_{0.5}\text{MnO}_3$ (c). The solid lines are a guide for the eye.

All three spectra consist of two rather broad peaks, the positions of their maxima are listed in Table II. For proper attribution of the peaks to each of the (O1)-(O5)¹¹ oxygen sites in the Bi-based manganites we first focus on $\text{Pr}_{0.5}\text{Ca}_{0.5}\text{MnO}_3$ which has the canonical CE-type magnetic structure at low temperature.

TABLE II: Zero-field ^{17}O NMR resonance frequencies for two oxygens sites in the ab -plane of $\text{Bi}_{0.5}\text{Sr}_{0.5}\text{MnO}_3$ (CE'-type magnetic structure), $\text{Bi}_{0.5}\text{Ca}_{0.5}\text{MnO}_3$ and $\text{Pr}_{0.5}\text{Ca}_{0.5}\text{MnO}_3$ (CE-type magnetic structure) at 4.2 K. The corresponding estimated values of $^{17}H_{loc} = 2\pi\nu/^{17}\gamma$ are shown in slashes. For $\text{Bi}_{0.5}\text{Sr}_{0.5}\text{MnO}_3$ the components of the magnetic moment μ_{ab} and μ_c of $\text{Mn}^{3+}/\text{Mn}^{4+}$ -ions at 4.2 K as well as β , the angle between $\mu(\text{Mn}^{3+})$ and the ab plane, were calculated using the ^{209}Bi and ^{17}O ZFNMR data (see text for details). For $\text{Bi}_{0.5}\text{Sr}_{0.5}\text{MnO}_3$ and $\text{Pr}_{0.5}\text{Ca}_{0.5}\text{MnO}_3$ these parameters were measured in Ref. 10 and Ref. 11 respectively.

Sample	$\text{Bi}_{0.5}\text{Sr}_{0.5}\text{MnO}_3$	$\text{Bi}_{0.5}\text{Ca}_{0.5}\text{MnO}_3$	$\text{Pr}_{0.5}\text{Ca}_{0.5}\text{MnO}_3$
$\nu(\text{O4})$ (MHz)/ $^{17}H_{loc}(\text{O4})$ (kOe)/	28/48.5/	31/54/	30/52/
$\nu(\text{O4})$ (MHz)/ $^{17}H_{loc}(\text{O4})$ (kOe)/	36/62/	40/69/	40/69/
μ (μ_B)	$ \mu_{ab}(\text{Mn}^{4+}) $	1.6	1.8
	$ \mu_c(\text{Mn}^{4+}) $	1.6	1.8
	$ \mu_{ab}(\text{Mn}^{3+}) $	2.1	2.5
	$ \mu_c(\text{Mn}^{3+}) $	1.4	1.15
β ($^\circ$)	33	25	0

The perfect CE-type CO/OO implies a zigzag arrangement of the ordered $e_g(3x^2-r^2)$ and $e_g(3y^2-r^2)$ orbitals of Mn^{3+} -ions in the ab -plane of the orthorhombic $Pbnm$ lattice, with the FM correlated magnetic moments in the zigzags. The neighboring zigzags are AF-coupled, the ordering in c -direction is also AF. Oxygen in the apical positions of MnO_6 octahedra is located between two Mn^{3+} -ions (O1-site, Fig. 3 in Ref. 11) or between two Mn^{4+} -ions (O2/O3-site). As shown in Ref. 3, the local magnetic field $^{17}H_{loc}$ is created mainly by the $2s$ spin polarization of oxygen transferred via the $e_g(\text{Mn})$ - $2s(\text{O})$ overlap from the neighboring Mn. This spin arrangement causes complete cancellation of the local magnetic field at the apical O1-O3 sites, and its corresponding ZFNMR line is out of the frequency range presented in Fig. 3. The O4-O5 sites correspond to the oxygens in the ab -plane. The oxygen (O4-site) participates in the AF-coupling of neighboring Mn^{4+} , Mn^{3+} from adjacent zigzags. The other oxygen (O5-site) is located inside a zigzag surrounded by two FM-coupled Mn^{4+} and Mn^{3+} ions.

The high-frequency peak in the ^{17}O ZFNMR spectrum is attributed to oxygen positioned in O5-sites whereas the low-frequency peak is presumably due to oxygen located in O4-sites. Indeed for oxygen in O5-site the transferred s -wave spin density is maximal since within the zigzag the lobe of the partially occupied $e_g(m_l = 0)$ orbital of Mn^{3+} -ion points toward this oxygen. Furthermore two neighboring Mn-ions are FM-correlated. For O4-site a rather large transferred hyperfine field is expected for the following reason. Although the Mn spins from adjacent zigzags are antiparallel, the O4-oxygen is "sandwiched" between Mn^{3+} and Mn^{4+} -ions with different spin values and different orbital occupations, i.e. with different covalency. So the transferred polarizations from these two Mn-ions should not compensate each other as they do for the apical oxygens (O1,O2/O3). It results in a substantial but smaller shift than for the O5-site. Moreover the transferred s -wave polarization from Mn^{4+} -ion is expected to be negative due to effects of covalent mixing with the empty e_g -orbitals. Indeed, the charge transfer

from the occupied O- $2s$ orbital to the empty e_g -orbital is spin-dependent since it is regulated by the intra-atomic exchange coupling with electrons on t_g -orbitals.

In the CE spin ordered state the transferred static s -wave polarization at the oxygen site may be expressed through the transferred spin densities $f_{s,3+}\mu(\text{Mn}^{3+})$ or $f_{s,4+}\mu(\text{Mn}^{4+})$ of the neighboring Mn (with $f_{s,3+} > 0$ and $f_{s,4+} < 0$), and the following expressions can be considered for $^{17}H_{loc}$ at the O5-site:

$$^{17}H_{loc}(\text{O5}) = (^{17}\gamma\hbar)^{-1}a(2s)\{f_{s,3+}\mu(\text{Mn}^{3+}) + f_{s,4+}\mu(\text{Mn}^{4+})\}, \quad (2)$$

and at the O4-site:

$$^{17}H_{loc}(\text{O4}) = (^{17}\gamma\hbar)^{-1}a(2s)\{0.25f_{s,3+}\mu(\text{Mn}^{3+}) - f_{s,4+}\mu(\text{Mn}^{4+})\}, \quad (3)$$

respectively. H_{loc} , $\mu(\text{Mn}^{3+})$ and $\mu(\text{Mn}^{4+})$ are vectors. The sign "+"/"-" in 2, 3 refers to the FM/AF spin correlations of the neighbor Mn^{3+} - and Mn^{4+} -ions. Here, $a(2s) = ^{17}\gamma\hbar H_{FC}(2s) = 0.0216 \text{ cm}^{-1}$ is the isotropic hyperfine coupling constant for oxygen ion.²¹ $H_{FC}(2s) = 1.1 \text{ MOe}$ is the corresponding hyperfine magnetic field due to the Fermi-contact interaction with the electron located on the $2s$ -orbital. Following Ref. 22, the corresponding isotropic spin density transferred to oxygen from neighboring Mn-ions may be defined with the factor $f_s = H_{loc}/2H_{FC}(2s)$.

Using the ^{17}O ZFNMR results and the neutron diffraction data from Ref. 11, listed in Table II, for $\text{Pr}_{0.5}\text{Ca}_{0.5}\text{MnO}_3$ we can quantify the factors f_s in Eqs. (2), (3) as: $f_{s,3+} = 0.0075$ and $f_{s,4+} = -0.0025$, which are somewhat less than $f_s = 0.01$ (Ref. 3) estimated in a similar way in the CD PM state for the very same sample.

Let us now consider $\text{Bi}_{0.5}\text{Sr}_{0.5}\text{MnO}_3$. As the degree of the spatial overlap of $e_g(\text{Mn})$ - $2s(\text{O})$ orbital decreases

rather slowly with the interatomic Mn-O distance in the series of manganites considered here, we assume that the ratio $f_{s,3+}/|f_{s,4+}|$ is not changed from $\text{Pr}_{0.5}\text{Ca}_{0.5}\text{MnO}_3$ to Bi-manganites. With this assumption and using the value of μ deduced from the refined neutron diffraction data for CE'-phase in $\text{Bi}_{0.5}\text{Sr}_{0.5}\text{MnO}_3$,¹⁰ equations (2) and (3) yield the values $f_{s,3+} = 0.009$ and $f_{s,4+} = -0.003$. Thus one can conclude that the admixture of the s -wave character to the e_g -wave function slightly increases in $\text{Bi}_{0.5}\text{Sr}_{0.5}\text{MnO}_3$ compared to $\text{Pr}_{0.5}\text{Ca}_{0.5}\text{MnO}_3$.

For $\text{Bi}_{0.5}\text{Ca}_{0.5}\text{MnO}_3$, there are no available refined staggered magnetization data. We have used the following assumptions in order to calculate the magnetic moments with the help of Eqs.(1)-(3):

- the same CE'-type magnetic structure as in $\text{Bi}_{0.5}\text{Sr}_{0.5}\text{MnO}_3$ takes place in $\text{Bi}_{0.5}\text{Ca}_{0.5}\text{MnO}_3$ at low temperature.

- the s -wave admixture to a character of the lone electron pair of the Bi^{3+} -ion, f_{6s} , is kept constant from Sr to Ca manganite.

As can be seen in Table II, from BiSrMnO to BiCaMnO to PrCaMnO the magnitude $|\mu|$ increases. Furthermore, it is accompanied by a decrease of μ_c which indicates a decreasing canting. Compared to the CE structure of $\text{Pr}_{0.5}\text{Ca}_{0.5}\text{MnO}_3$, the CE' structure of the Bi-based samples may be related to a stronger interplane coupling and/or a specific anisotropy of the Jahn-Teller distortion along c axis. Our results show that the CE'-type structure in $\text{Bi}_{0.5}\text{Sr}_{0.5}\text{MnO}_3$ is more pronounced than in $\text{Bi}_{0.5}\text{Ca}_{0.5}\text{MnO}_3$.

C. ^{17}O NMR in the paramagnetic charge-disordered and charge-ordered states

Figures 4 (a,b) show the ^{17}O NMR spectra measured at different temperatures on $\text{Bi}_{0.5}\text{Ca}_{0.5}\text{MnO}_3$ and $\text{Bi}_{0.5}\text{Sr}_{0.5}\text{MnO}_3$ in the PM state. The spectra were obtained at $H \approx 90$ kOe above $T = 320$ K and at $H \approx 120$ kOe below 320 K. The comparison (not shown) of the spectra obtained with both fields around 300K demonstrates the negligible effect of the quadrupolar interaction. For comparison we reproduce in Fig. 4 (c) the ^{17}O NMR spectra ($H \approx 70$ kOe) of $\text{Pr}_{0.5}\text{Ca}_{0.5}\text{MnO}_3$ in the PM state.³ All the spectra were taken when cooling the samples from the highest temperature indicated in Fig. 4 (a-c) to avoid any hysteresis. According to resistivity data,^{23,24} cooling our Bi-samples in the external magnetic field indicated above does not suppress the CO-transition.

For all compounds, in the CD-state above T_{CO} the ^{17}O spectrum consists of a single line. With decreasing temperature its shift ^{17}K increases following the Curie-Weiss law $^{17}K \sim (T - \theta)^{-1}$ with positive θ indicating the presence of FM electron correlations of Mn: $\theta = 250(40)$ K in $\text{Bi}_{0.5}\text{Sr}_{0.5}\text{MnO}_3$, $170(10)$ K in $\text{Bi}_{0.5}\text{Ca}_{0.5}\text{MnO}_3$ and $130(20)$ K in $\text{Pr}_{0.5}\text{Ca}_{0.5}\text{MnO}_3$.³

We have used static magnetic susceptibility χ data for

$\text{Bi}_{0.5}\text{Ca}_{0.5}\text{MnO}_3$ ⁵ and $\text{Bi}_{0.5}\text{Sr}_{0.5}\text{MnO}_3$ ⁹ to estimate the corresponding s -wave spin density transferred to oxygen from neighboring Mn in the CD state. The slope of ^{17}K vs χ plot corresponds to the local magnetic field $^{17}H_{loc} = \mu_B \Delta K / \Delta \chi = 12.0(5)$ kOe/ μ_B ($\text{Bi}_{0.5}\text{Sr}_{0.5}\text{MnO}_3$) and $^{17}H_{loc} = 12.4(5)$ kOe/ μ_B ($\text{Bi}_{0.5}\text{Ca}_{0.5}\text{MnO}_3$). For $\text{Pr}_{0.5}\text{Ca}_{0.5}\text{MnO}_3$ we refined the estimation of $^{17}H_{loc} = 7.1(3)$ kOe/ μ_B in an accurate ^{17}O NMR study performed at 120 kOe as compared to the earlier published value.³ In comparison to $\text{Pr}_{0.5}\text{Ca}_{0.5}\text{MnO}_3$, the increase of $^{17}H_{loc}$ in the Bi-based manganites evidences a larger $e_g(\text{Mn})-2s(\text{O})$ admixture.

For $\text{Pr}_{0.5}\text{Ca}_{0.5}\text{MnO}_3$, $T_{crit} = 250$ K.¹¹ T_{crit} is defined as the temperature at which the transition from the high- T cubic $Pm\bar{3}m$ to the orthorhombic $Pbnm$ structure occurs and thus it is related to the onset of orbital ordering. As seen in Fig. 4 (c), below $T \approx 250$ K the ^{17}O spectrum of $\text{Pr}_{0.5}\text{Ca}_{0.5}\text{MnO}_3$ substantially broadens and splits into three lines as the temperature approaches T_N . According to Ref. 3, the low-frequency line is attributed to apical oxygens while the two other lines corresponding to the shift $^{17}K = 40\%$ and 55% are attributed to the oxygens located in ab -plane (O4- and O5-site, respectively). As said before, the magnetic shift ^{17}K of the apical line is greatly reduced due to the vanish of the local field. The NMR signal of the apical oxygen appears at a characteristic temperature $T_{CO,nmr}$, below which AF spin correlations between ab -layers occur. It is not surprising that $T_{CO,nmr}$ coincides with T_{crit} since the localization of the itinerant electrons at e_g -orbitals should manifest itself both in the appearance of AF spin correlations between ab -layers and in the cooperative Jahn-Teller distortions in the MnO_6 -octahedra sublattice.

For $\text{Bi}_{0.5}\text{Ca}_{0.5}\text{MnO}_3$, the ^{17}O NMR spectra drastically change below $T_{CO,nmr}$, indicated by the narrow grey stripe in Fig. 4 (a). Moreover, the line shape shown in Fig. 5 becomes extremely sensitive to t - the time delay between the rf -exciting pulses. The solid curve shows the echo intensity vs frequency (ν) measured at short time delay $t = 12 \mu\text{s}$, while the open squares indicate the echo intensity observed at large delay, $t=100 \mu\text{s}$. By measuring the rate of the echo decay ($^{17}T_2^{-1}$) at several representative points of the spectrum, we have reconstructed the high-frequency part of the spin-echo spectrum at $t = 0$ (solid squares), its intensity being the difference between the spectra measured with $t = 12 \mu\text{s}$ and $100 \mu\text{s}$. It worth noting that, $T_{CO,nmr}$ (Fig. 5) is consistent with $T_{crit} = 335(30)$ K (Ref. 5) defined as the temperature of the cubic-to-orthorhombic structural transition. With further decrease of temperature a substantial part of the high-frequency tail becomes undetectable due to a too small value of T_2 ($^{17}T_{2,min} \approx 5 \mu\text{s}$). Although only $\text{Bi}_{0.5}\text{Ca}_{0.5}\text{MnO}_3$ is shown in Fig. 5, a very similar $^{17}T_2$ effect on the high-frequency tail of the ^{17}O spin-echo spectrum occurs in the CO-phase of $\text{Bi}_{0.5}\text{Sr}_{0.5}\text{MnO}_3$ below $T_{CO,nmr}$.

In order to understand why in contrast to $\text{Pr}_{0.5}\text{Ca}_{0.5}\text{MnO}_3$ below $T_{CO,nmr}$, the high-frequency part

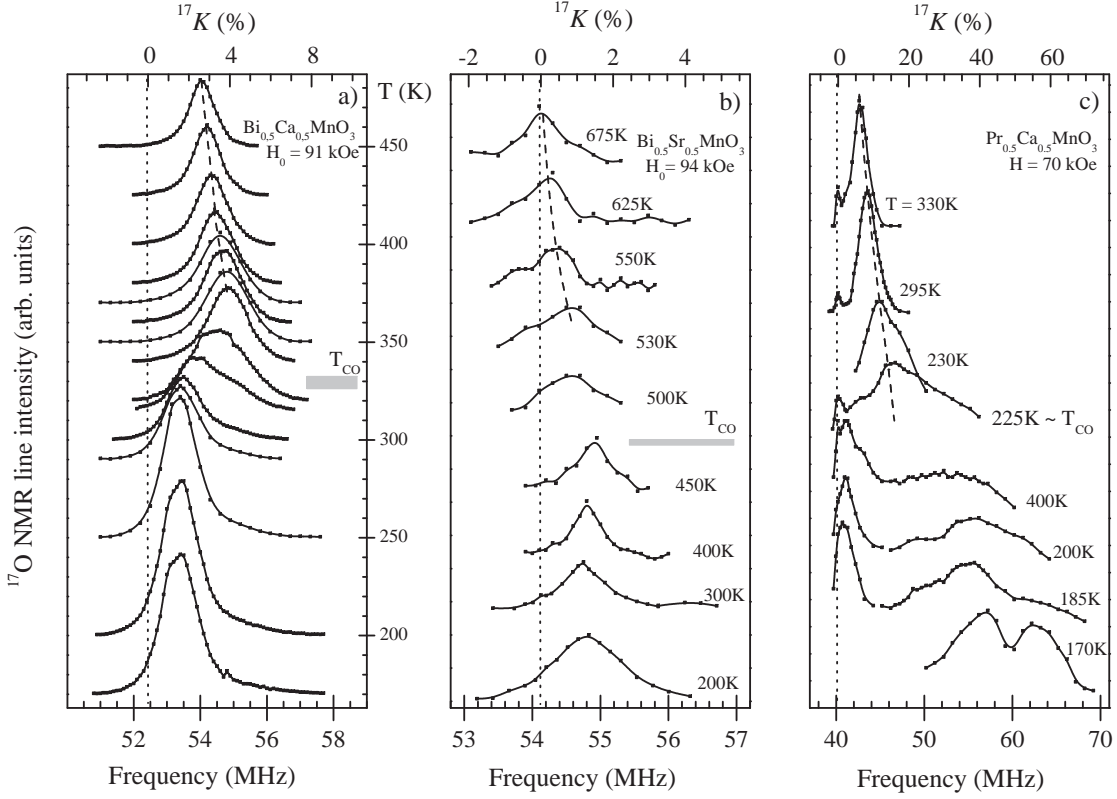


FIG. 4: ^{17}O NMR spectra measured in the paramagnetic state of $\text{Bi}_{0.5}\text{Ca}_{0.5}\text{MnO}_3$ (a), $\text{Bi}_{0.5}\text{Sr}_{0.5}\text{MnO}_3$ (b), and $\text{Pr}_{0.5}\text{Ca}_{0.5}\text{MnO}_3$ (c).³ The position of the Larmor frequency ($K = 0$) is shown by dotted vertical line. The grey narrow stripe indicates T_{CO} - critical temperature of the charge ordering.

of the spectrum in $\text{Bi}_{0.5}\text{Ca}_{0.5}\text{MnO}_3$ and $\text{Bi}_{0.5}\text{Sr}_{0.5}\text{MnO}_3$ is difficult to be detected, we have studied $^{17}\text{T}_2$ thermal behaviour in both CO phases, paramagnetic and antiferromagnetic. $^{17}\text{T}_2^{-1}$, measured in $\text{Bi}_{0.5}\text{Ca}_{0.5}\text{MnO}_3$ on the low frequency peak of the ZF NMR spectrum (O4 site, $\nu = 30$ MHz; see Fig. 3 b) is shown by up-triangles in Fig. 6. It evidences a divergent increase with temperature. The data set shown by the closed and open squares correspond to $^{17}\text{T}_2^{-1}$ measured on the apical line in $\text{Bi}_{0.5}\text{Sr}_{0.5}\text{MnO}_3$ and in $\text{Bi}_{0.5}\text{Ca}_{0.5}\text{MnO}_3$ respectively. For the apical line there is also an enhancement of $^{17}\text{T}_2^{-1}$ which occurs in the same temperature range for both Bi-based compounds. Furthermore, though weaker, this enhancement occurs in the same temperature range as for O4 site. The detailed study of the Mn-spin fluctuation probed by $^{17}\text{T}_2^{-1}$ will be discussed elsewhere. Here we just point out the T_2 which is more than one order of magnitude shorter than in $\text{Pr}_{0.5}\text{Ca}_{0.5}\text{MnO}_3$ and thus the difference in the Mn spin fluctuation in the Bi-based manganites compared to $\text{Pr}_{0.5}\text{Ca}_{0.5}\text{MnO}_3$.

The thermal behaviour of $^{17}\text{T}_2^{-1}$ explains why in the

Bi-based compounds the high frequency lines corresponding to O4 and O5, which are not detected in the PM CO phase ($^{17}\text{T}_2^{-1} > 100$ ms⁻¹), are well observed at very low temperature. Indeed, they appear at $T = 4.2$ K as a two-peaked spectrum in zero field NMR (Figs. 3 b; 3 c) and as a very broad high-frequency tail at $T = 15$ K for the ^{17}O NMR spectrum measured at 12 T as shown in Fig. 7 for $\text{Bi}_{0.5}\text{Sr}_{0.5}\text{MnO}_3$.

D. ^{17}O NMR in the antiferromagnetic charge-ordered state

In this section we consider the peculiarities in the ^{17}O NMR spectrum measured in the antiferromagnetic charge-ordered state of $\text{Bi}_{0.5}\text{Sr}_{0.5}\text{MnO}_3$ far below the Neel temperature, when the development of the static spin correlations is completed. We show that our analysis of the spectrum yields some constraints for the theoretical model of the CO phase in manganites.

The ^{17}O NMR spectra of $\text{Pr}_{0.5}\text{Ca}_{0.5}\text{MnO}_3$ and

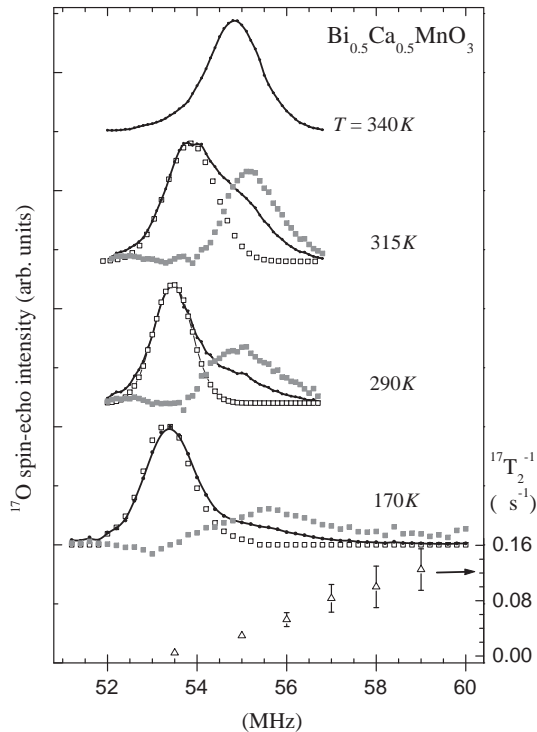


FIG. 5: Evolution of the ^{17}O spectrum pattern for $\text{Bi}_{0.5}\text{Ca}_{0.5}\text{MnO}_3$ showing the onset of the splitting into two lines when cooling below T_{CO} from the charge-disordered to the charge-ordered paramagnetic phase. The solid line shows the echo intensity vs frequency measured with the time delay $t = 12 \mu\text{s}$ between the rf -exciting pulses; open squares indicate the echo intensity measured with $t = 100 \mu\text{s}$. Solid squares are the normalized high-frequency part of the spectra obtained by reconstructing at $t = 0$ the difference between the echo intensities measured with $12 \mu\text{s}$ and $100 \mu\text{s}$. The open up-triangles are the $^{17}T_2^{-1}$ data measured between 53 MHz and 59 MHz at $T = 170 \text{ K}$.

$\text{Bi}_{0.5}\text{Sr}_{0.5}\text{MnO}_3$ are shown in Figure 7. The intensity is a result of two corrections. First, the intensity being related to the T_2 value at a given frequency, the spectra were recalculated for a time delay $t = 0$, between exciting rf -pulses. Second, the spectral intensity is proportional to the intensity of the echo signal, ^{17}Int , normalized by the factor ν^{-2} at each frequency point ν of the spectrum. Thus, it yields directly the fraction of oxygen at (O1-O5) sites, which contributes to the echo-signal at a given frequency point $^{17}K = (\nu - \nu_0)/\nu_0$.

For $\text{Pr}_{0.5}\text{Ca}_{0.5}\text{MnO}_3$ the spectrum was measured in the same magnetic field of 70 kOe as in the CO paramagnetic phase shown in Fig. 4 c. The narrow line-A is due to oxygen in the apical (O1-O3) sites, while the broad line-(B+C) originates from oxygen in the ab -plane (O4-O5 sites). The unresolved pattern of this line is a result of additional magnetic broadening below $T_N = 170 \text{ K}$.

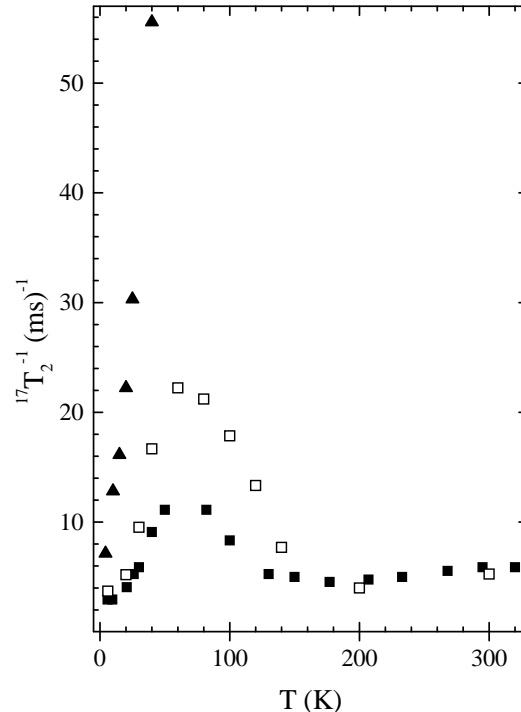


FIG. 6: Thermal behaviour of ^{17}O spin-spin relaxation rate, $^{17}T_2^{-1}$, in the charge ordered, paramagnetic and antiferromagnetic phases for the two Bi-based manganites. $^{17}T_2^{-1}$ of the oxygen in the ab -plane (O4-site) measured with $H_{ext} = 0$ (Δ) and of the apical oxygen (\blacksquare) measured with $H_{ext} = 50 \text{ kOe}$ in $\text{Bi}_{0.5}\text{Ca}_{0.5}\text{MnO}_3$. For $\text{Bi}_{0.5}\text{Sr}_{0.5}\text{MnO}_3$, $^{17}T_2^{-1}$ of the apical oxygen ($H_{ext} = 120 \text{ kOe}$) is shown by open squares.

The ratio of the integral NMR line intensities $r_{nmr} = (I_A/I_{B+C}) = 0.96(10)$ is very close to the structural ratio $r_{struct} = 2 : 2$ of the oxygen atoms occupying the apical sites and those placed in the ab -plane.

It is worth emphasizing that this estimate of $r_{nmr} \approx r_{struct} = 1$ allows the scenario of the site-centered CE-type charge ordering which develops in $\text{Pr}_{0.5}\text{Ca}_{0.5}\text{MnO}_3$ among the ions of different valence ($\text{Mn}^{3.5+\delta}/\text{Mn}^{3.5-\delta}$).^{12,13,14} Indeed, such a value is expected only for the magnetic structure of the conventional CE-type, i.e., in the ionic model.

Let us address now to the ^{17}O NMR spectrum of $\text{Bi}_{0.5}\text{Sr}_{0.5}\text{MnO}_3$ measured at 120 kOe and 15 K. The essential feature of the spectrum is that the gravity center of the broad high-frequency line is substantially shifted towards smaller ^{17}K , compared with the rather well resolved spectrum of $\text{Pr}_{0.5}\text{Ca}_{0.5}\text{MnO}_3$. The integral intensity of line-A is approximately twice as larger as that of the broad line integrated in the range of ^{17}K above

15%. The corresponding ratio $r_{nmr} \approx 2$ is a clear indication that in the CO state of $\text{Bi}_{0.5}\text{Sr}_{0.5}\text{MnO}_3$ a sizeable fraction of oxygen located in the ab -plane experiences a reduced local field. The reduction of this local field is mainly controlled by the occupancy of the $e_g(\text{Mn})$ orbital. The inequality $r_{nmr} > r_{struct} = 1$ is expected for the bond-centered models of CO suggested for half doped manganites.^{14,15,16} In these OO models there is a reduction of $^{17}\text{H}_{loc}$ at some oxygen sites in the ab -plane. As an example, for the Zener polaron state,¹⁵ the local field should vanish at the oxygen atom located between the AF-correlated adjacent dimers of $\text{Mn}^{3.5+}$. Thus, we incline to consider the $e_g(\text{Mn})$ orbital ordering in the CO state of $\text{Bi}_{0.5}\text{Sr}_{0.5}\text{MnO}_3$ in the frame of the CO bond-centered models. It's worth noting that for the CE'-type magnetic structure, the Mn magnetic moments do not lie in the ab -plane and the c -component $\mu_c \neq 0$. In the CE'-type structure, the conventional theoretical treatment of the OO order in the frame of 2D-models is not appropriate approach to consider in join the e_g -orbital and spin order, observed in $\text{Bi}_{0.5}\text{Sr}_{0.5}\text{MnO}_3$ at low T .²⁶ It should be required to involve the interplane couplings into consideration.

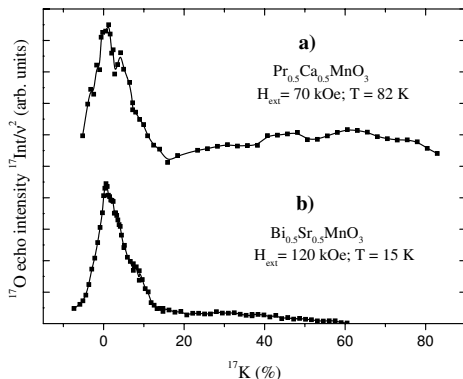


FIG. 7: ^{17}O NMR spectrum in the antiferromagnetic charge-ordered phase of $\text{Pr}_{0.5}\text{Ca}_{0.5}\text{MnO}_3$ (a) and $\text{Bi}_{0.5}\text{Ca}_{0.5}\text{MnO}_3$ (b). The spectra were obtained at the field cooled samples.

IV. CONCLUSION

We have studied the development of the Mn electron spin correlations in two half-doped Bi-based manganites $\text{Bi}_{0.5}\text{Sr}_{0.5}\text{MnO}_3$ and $\text{Bi}_{0.5}\text{Ca}_{0.5}\text{MnO}_3$ in going from the charge-disorder paramagnetic phase to the charge-ordered antiferromagnetic phase and compared it to $\text{Pr}_{0.5}\text{Ca}_{0.5}\text{MnO}_3$.

In the Bi-based manganites, the ZF NMR results show that the unusually large local magnetic field $^{209}\text{H}_{loc}$ strongly favors the dominant $6s^2$ character of the lone electron pair located at the Bi^{3+} -ions in both compounds. The mechanism which connects the s character of the

lone pairs of Bi^{3+} to the high value of T_{CO} is still not clarified.

Compared to $\text{Bi}_{0.5}\text{Sr}_{0.5}\text{MnO}_3$ the small decrease of $^{209}\text{H}_{loc}$ in $\text{Bi}_{0.5}\text{Ca}_{0.5}\text{MnO}_3$ is attributed to a slight difference in the magnetic structure of the CE'-type spin order presumed for both manganites rather than to a change of the wave character of the lone electron pair as it was suggested for Ca-doped oxide in Ref. 6. Our ^{17}O and ^{209}Bi ZF NMR data show that, more probably, the difference in the observed $^{209}\text{H}_{loc}$ is due to a decrease in the canting of the staggered magnetic moments of Mn^{3+} -ions in $\text{Bi}_{0.5}\text{Ca}_{0.5}\text{MnO}_3$ compared to $\text{Bi}_{0.5}\text{Sr}_{0.5}\text{MnO}_3$. For $\text{Bi}_{0.5}\text{Ca}_{0.5}\text{MnO}_3$ it would be interesting to compare the distribution of staggered magnetization deduced from NMR data with neutron diffraction data that are still not available. It would help us to make more definite conclusion on the role of the stereoactivity of the Bi^{3+} lone electron pair in the high value of T_{CO} of the $\text{Bi}_{1-x}\text{Sr}_x\text{MnO}_3$ ($x \leq 0.5$) manganites.

Comparing the evolution of ^{17}O NMR spectra from CD to CO PM state, we have demonstrated the qualitative modification of the spectra at the temperature of order-disorder transition, below which the localization of itinerant e_g -electrons manifests itself in two specific phenomena, namely, the appearance of interlayer AF spin correlations and the cooperative Jahn-Teller distortions in the MnO_6 -octahedra sublattice. Indeed, this is well demonstrated by the proximity of $T_{CO,nmr}$, below which AF interlayer spin correlations occur, to T_{crit} , at which structural changes occur. This ^{17}O NMR study demonstrates that the line corresponding to the apical oxygens is a unique local tool to study the development of the interlayer Mn-Mn spin correlations. Indeed for all three manganites this line occurs as soon as the charge-ordered phase develops on decreasing the temperature below T_{CO} . It also could be a useful local probe to study the influence of a magnetic field or an external pressure on the phase diagram.

In the CO state, $^{17}T_2$ is much shorter in the high frequency part of the spectrum, which corresponds to oxygens in the ab -plane in both Bi-manganites, compared to $\text{Pr}_{0.5}\text{Ca}_{0.5}\text{MnO}_3$. This great increase of the rate of the ^{17}O spin-echo decay can be interpreted in the following way. The time-dependent fluctuations of the local field can greatly increase the spin-spin relaxation rates of these oxygens. The T_2 effect becomes important when the characteristic correlation time of the Mn electron spin fluctuations t_c is comparable to $1/\omega$, where ω is the Larmor precession of the ^{17}O nuclear spin in the magnetic field. The maximum of $^{17}T_2^{-1}$ is expected near $t_c(T) = 1/\omega$. Thus, compared with the spin fluctuation spectrum for the CE-ordered $\text{Pr}_{0.5}\text{Ca}_{0.5}\text{MnO}_3$, in Bi-compounds the spectral intensity of the Mn electron spin fluctuations is shifted to low frequencies, comparable to ω .

It is shown on an example of $\text{Pr}_{0.5}\text{Ca}_{0.5}\text{MnO}_3$ and $\text{Bi}_{0.5}\text{Sr}_{0.5}\text{MnO}_3$, that the analysis of the ^{17}O spectrum imposes some constraints for the theoretical descrip-

tion of the charge ordered phase in the AF state of manganites. In this analysis the relative intensity of the low and high frequency ^{17}O lines is calculated and compared to the site-centered and bond-centered models. As the result the fine structure of the ^{17}O spectrum in $\text{Pr}_{0.5}\text{Ca}_{0.5}\text{MnO}_3$ is well consistent with predictions of the site-centered model of CO among the ions ($\text{Mn}^{3.5+\delta}/\text{Mn}^{3.5-\delta}$). While ^{17}O NMR analysis of the Mn-Mn spin correlations developed in the AF state of $\text{Bi}_{0.5}\text{Sr}_{0.5}\text{MnO}_3$ indicates on the bond-centered models of CO as the more appropriate approach for the Bi-based

manganite.

Acknowledgments

We are very grateful to Dr. A.Inyushkin for ^{17}O isotope enrichment. The work is supported partly by Russian Foundation for Basic Research (Grants 02-02-16357a) as well as by CRDF PR 2355.

-
- ¹ R. Kajimoto, T. Kakeshita, Y. Oohara, H. Yoshizawa, Y. Tomioka, and Y. Tokura, Phys.Rev. B **58**, R11837 (1998).
- ² H. L. Liu, S. L. Cooper, and S.-W. Cheong, Phys. Rev. Letters **81**, 4684 (1998).
- ³ A. Yakubovskii, A. Trokiner, S. Verkhovskii, A. Gerashenko, and D. Khomskii, Phys.Rev. B **67**, 064414 (2003).
- ⁴ C. Zener, Phys.Rev. **82**, 403 (1951).
- ⁵ V. Bokov, N. Grigoryan, and M. Bryzhina, Phys. Status Solidi **20**, 745 (1967).
- ⁶ J. Garcia-Munoz, C. Frontera, M. Aranda, A. Llobet, and C. Ritter, Phys.Rev. B **63**, 064415 (2001).
- ⁷ P. Beran, S. Malo, C. Martin, A. Maignan, M. Nevrieva, M. Hervieu, and B. Raveau, Solid State Sci. **4**, 917 (2002).
- ⁸ A. Frontera, J. Garcia-Munoz, M. Aranda, M. Hervieu, C. Ritter, L. Manosa, X. Capdevila, and A.Galleja, Phys. Rev. B **68**, 134408 (2003).
- ⁹ J. Hejtmanek, K. Knizek, Z. Jirak, M. Hervieu, C. Martin, M. Nevrieva, and P. Beran, J. Appl. Phys. **93**, 7370 (2003).
- ¹⁰ C. Frontera, J. Garcia-Munoz, M. Aranda, C. Ritter, A. Llobet, M. Respaud, and J. Vanacken, Phys.Rev. B **64**, 054401 (2001).
- ¹¹ Z. Jirak, F. Damay, M. Hervieu, C. Martin, B. Raveau, G. Andre, and F.Bouree, Phys.Rev. B **61**, 1181 (2000).
- ¹² E. Wollan and W. Koeler, Phys.Rev. **100**, 543 (1955).
- ¹³ Z. Jirak, S. Krupicka, Z. Simsa, M. Dlouha, and Z. Vratislav, J. Magn. Magn. Mater. **53**, 153 (1985).
- ¹⁴ D. Efremov, J. van den Brink, and D. Khomskii, cond-mat/0306651 (2003).
- ¹⁵ A. Daoud-Aladine, J. Rodriguez-Carvajal, L. Pinsard-Gaudart, M. Fernandez-Diaz, and A. Revcolevschi, Phys. Rev. Letters **89**, 97205 (2002).
- ¹⁶ D. Efremov, J. van den Brink, and D. Khomskii, Nature: materials **3**, 853 (2004).
- ¹⁷ K. Kumagai, A. Iwai, Y. Tomioka, H. Kuwahara, Y. Tokura, and A.Yakubovskii, Phys. Rev. B **59**, 9 (1999).
- ¹⁸ Y. Yoshinari, P. Hammel, J. Tompson, and S.-W. Cheong, Phys. Rev. B **60**, 9275 (1999).
- ¹⁹ G. Allodi, R. D. Renzi, F. Licci, and M. W. Pieper, Phys. Rev. Letters **81**, 4736 (1998).
- ²⁰ G. Carter, L. Bennett, and D. Kahan, *Metallic Shifts in NMR, in Progress in Material Science, edited by B. Chalmers, J.W. Christian, T.B. Massalski* (Pergamon Press, Oxford, 1977), p. 33.
- ²¹ S. Fraga, J. Karwowski, and K. Saxena, *Handbook of Atomic Data* (Elsevier Scientific Pub., Amsterdam, 1976).
- ²² R. Shulman and V. Jaccarino, Phys. Rev. **108**, 1219 (1957).
- ²³ Y. Tomioka, A. Asamitsu, H. Kuwahara, Y. Morimoto, and Y. Tokura, Phys.Rev. B **53**, R1689 (1996).
- ²⁴ A.Kirste, M. Goiran, M. Respaud, J. Vanaken, J. M. Broto, H. Rakoto, M. von Ortenberg, C. Frontera, , and J. L. Garcia-Munoz, Phys. Rev. B **67**, 134413 (2003).
- ²⁵ In both Bi-based manganites the ZFNMR spectrum shows a partial overlap of the low-frequency tail of the ^{209}Bi signal with the ^{17}O spectrum (see Fig. 2 and 3). The spin-echo spectra of ^{17}O (Fig. 3) were obtained by applying a pulse sequence, which parameters were adjusted to obtain the maximum ratio $I = {}^{17}\text{Int}/{}^{209}\text{Int}$ where ${}^{17}\text{Int}$ and ${}^{209}\text{Int}$ are the spin echo intensities. In these conditions the ratio I exceeds 10. Furthermore, we have compared the ZFNMR spectra measured in the ^{17}O enriched and in a natural $\text{Bi}_{0.5}\text{Ca}_{0.5}\text{MnO}_3$ sample. The latter is a non-enriched fraction of the very same $\text{Bi}_{0.5}\text{Ca}_{0.5}\text{MnO}_3$ material. Its ^{209}Bi ZFNMR spectrum is shown on the top panel of Fig.2. From this comparison, we found that the difference of the spectra reproduces rather well the two-peaks line shape and each peak position of the ^{17}O ZFNMR spectrum presented on Fig. 3 b.
- ²⁶ For the CE' magnetic structure of the $\text{Mn}^{3+/4+}$ ions ordered in the ab-plane like a checkerboard (see Fig. 2 a in Ref. 10) one might expect $r_{nmr} < 1$, since an apical oxygen surrounded by Mn^{3+} ions (see Fig. 1 c) experiences the local field not cancelled along c -axis.